The Role of Inflammation Resolution Speed in Airway Smooth Muscle Mass Accumulation in Asthma: Insight from a Theoretical Model

Igor L. Chernyavsky[1]*, Huguette Croisier[1], Lloyd A. C. Chapman[2], Laura S. Kimpton[2], Jonathan E. Hiorns[1], Bindi S. Brook[1], Oliver E. Jensen[3], Charlotte K. Billington[4], Ian P. Hall[4], Simon R. Johnson[4]

1 School of Mathematical Sciences, University of Nottingham, Nottingham, United Kingdom, 2 Mathematical Institute, University of Oxford, Oxford, United Kingdom, 3 School of Mathematics, University of Manchester, Manchester, United Kingdom, 4 Department of Therapeutics and Molecular Medicine, University of Nottingham, Nottingham, United Kingdom

Abstract

Despite a large amount of *in vitro* data, the dynamics of airway smooth muscle (ASM) mass increase in the airways of patients with asthma is not well understood. Here, we present a novel mathematical model that describes qualitatively the growth dynamics of ASM cells over short and long terms in the normal and inflammatory environments typically observed in asthma. The degree of ASM accumulation can be explained by an increase in the rate at which ASM cells switch between non-proliferative and proliferative states, driven by episodic inflammatory events. Our model explores the idea that remodelling due to ASM hyperplasia increases with the frequency and magnitude of these inflammatory events, relative to certain sensitivity thresholds. It highlights the importance of inflammation resolution speed by showing that when resolution is slow, even a series of small exacerbation events can result in significant remodelling, which persists after the inflammatory episodes. In addition, we demonstrate how the uncertainty in long-term outcome may be quantified and used to design an optimal low-risk individual anti-proliferative treatment strategy. The model shows that the rate of clearance of ASM proliferation and recruitment factors after an acute inflammatory event is a potentially important, and hitherto unrecognised, target for anti-remodelling therapy in asthma. It also suggests new ways of quantifying inflammation severity that could improve prediction of the extent of ASM accumulation. This ASM growth model should prove useful for designing new experiments or as a building block of more detailed multi-cellular tissue-level models.

Introduction

Asthma is a chronic inflammatory disease, characterised by acute inflammatory events during which antigen exposure triggers the production or recruitment of inflammatory cells (mast cells, T-cells, eosinophils, etc.). These cells secrete inflammatory mediators and growth factors which induce acute inflammation and bronchoconstriction of an airway wall over the short term (i.e. minutes to hours) and its remodelling over the long term (i.e. days to months) [1,2].

Airway smooth muscle (ASM) mass increase is an important aspect of both airway remodelling and hyper-responsiveness [3,4]. ASM mass accumulation can be triggered by multiple factors, including inflammation and bronchoconstriction (see Fig. 1). There is ongoing debate regarding the relative contributions of ASM cell proliferation, hypertrophy and recruitment (e.g. via differentiated fibroblasts and myofibroblasts) in asthmatic airways [5–7]. A large number of inflammatory mediators are associated with ASM proliferation *in vitro*, and infiltrating inflammatory cells are a feature of asthma [8]. However, the precise role of these factors in ASM mass accumulation *in vivo* is not well understood

[7]. The many factors involved in airway remodelling, combined with the difficulties and risks of invasive airway biopsies in patients with asthma (particularly during exacerbations) and the lack of consensus on animal models and *in vitro* systems, have motivated research on understanding ASM mass increase by non-invasive means, including mathematical modelling [9,10].

Quantitative data on various aspects of lung function and airway inflammation can be used to inform mathematical models. These include [11]: (i) bronchial biopsies, which reveal the amount of airway wall remodelling and allow one to estimate the percentage of proliferating and apoptotic ASM cells; (ii) analyses of inflammatory mediators present in blood and airway sputum differential cell counts; (iii) exhaled nitric oxide concentration measurements, and (iv) lung function tests, in particular forced expiratory volume in one second (FEV_1) recordings. The most direct quantitative information on ASM accumulation, provided by bronchial biopsies, is very limited due to the invasive nature of this procedure. Lung function and inflammatory biomarker measures, however, are more readily performed.
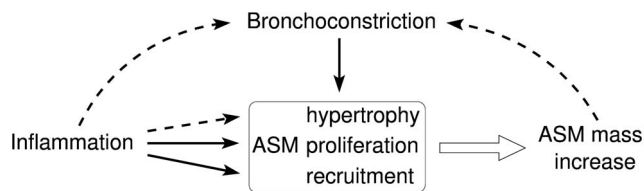
Figure 1. Possible pathways of chronic ASM mass accumulation in asthma (solid lines indicate the mechanisms included in the mathematical model).
doi:10.1371/journal.pone.0090162.g001

In this paper, we focus on developing a simple theoretical model of long-term ASM hyperplasia (proliferation and recruitment) via inflammatory pathways, which has the potential to integrate the information from airway biopsies and inflammatory biomarkers. This model allows possible ASM accumulation scenarios to be explored and suggests possible new targets for diagnosis and prevention of ASM remodelling.

Methods

Model formulation and assumptions

We employ a simple model, schematised in Fig. 2(a), in which we assume ASM cells are either in a proliferative state (which also accounts for recruitment) or a non-proliferative state [12,13]. These are respectively characterized by time-dependent population sizes in an airway wall $p(t)$ and $c(t)$, and the total ASM cell population is denoted $s(t) = p + c$. In the following, "proliferation" refers to both cell replication and recruitment, i.e. it is used as a synonym for hyperplasia.

Switching between the two states is governed by the rates λ_{cp} and λ_{pc}. Proliferation of the p-subpopulation is assumed to follow a logistic law (see S1.1 in Materials S1), with proliferation rate λ_p, and maximal population size ("total capacity") V. The latter implicitly includes the effect of spatial constraints in the airway wall, as well as p-cell apoptosis. For convenience, in the following, all population sizes are normalised by V, so that the maximum total cell population size is $s = 1$. The apoptosis rate of the c-subpopulation, λ_a, is assumed to be much smaller than λ_p ($\lambda_a \ll \lambda_p$) [14]. We also assume that ASM cells do not remain in the proliferative state for a long time ($\lambda_{pc} \gg \lambda_p$).

A third variable, the *inflammatory status* $\mu(t)$, modulates the switching rate λ_{cp} of ASM cells between the non-proliferative and proliferative states (Fig. 2(a,b)). We assume that μ changes in response to environmental stimuli of average magnitude a and average frequency ω and decays with a rate λ_d (the inflammation clearance rate), as illustrated in Fig. 2(c) (see Materials S1 for governing equations). The terminology "inflammatory status" refers in this work to all possible downstream triggers of ASM mass increase, including bronchoconstriction [15,16] (see Fig. 1). Similarly, "exacerbation", or "acute inflammatory event", refers to any substantial rapid increase in the inflammatory status (whether or not this leads to patient hospitalisation).

The way the switching rate λ_{cp} varies as a function of μ, relative to the other rate parameters, is depicted in Fig. 2(b). It is characterised by two thresholds, μ_1 and μ_2, such that:

(1) For $\mu < \mu_1$ (the "healthy" case), λ_{cp} is sufficiently small ($\lambda_a \ll \lambda_{cp} \ll \lambda_p \ll \lambda_{pc}$) for the total ASM cell population to remain approximately stationary (case (1) in Fig. 2(b,d));

(2) For $\mu_1 \leq \mu < \mu_2$ ("mild" inflammation), λ_{cp} is elevated ($\lambda_a \ll \lambda_{cp} \approx \lambda_p \ll \lambda_{pc}$) such that the ASM cell population increases

on a slow 'remodelling' timescale ($t \approx T \gg 1/\lambda_p$, i.e. weeks to months; case (2) in Fig. 2(b,d));

(3) For $\mu \geq \mu_2$ ("severe" inflammation), λ_{cp} is increased further ($\lambda_a \ll \lambda_p \ll \lambda_{cp} \approx \lambda_{pc}$), allowing ASM cell population to increase on a fast 'proliferation' timescale ($t \approx 1/\lambda_p$, i.e. days to weeks; case (3) in Fig. 2(b,d)).

Table 1 gives the literature-based values of the model parameters.

We consider both periodic and irregular timing of exacerbation events in the simulations. Given the irregular nature of events that are likely to occur in reality, we seek to explore the impact of this randomness on ASM remodelling. We run a large number of simulations ($N = 1000$), in each of which we allow exacerbation events to occur randomly according to a Poisson process. The resulting fold-increase in ASM mass at 300 days is recorded for each simulation. This may be interpreted as 1000 possible outcomes in an individual subject given the same average characteristics (magnitude and mean frequency) from a given initial state. The outcomes plotted as a histogram then allow quantification of the likelihood of developing severely or moderately remodelled airways. This is analogous to a weather forecast in which a number of different possible outcomes are determined from a given current state.

Solution techniques

We use a combination of analytical techniques (multi-timescale analysis) and computer simulations (with *ode45* MATLAB Runge-Kutta solver) to characterise the dynamics of the ASM cell population growth (see S1.2 in Materials S1 for technical details).

Results

Survey of ASM growth scenarios

The fundamental properties of the model are illustrated in Figure 2(d), where the effect of successive stepwise increases and decreases of the inflammation status μ through the three inflammation regimes (Fig. 2b) is simulated. Over the considered time span (about 1 month in each regime), only severe inflammation (case (3)) leads to substantial growth of the ASM cell population. In the other two cases, the non-proliferative phenotype is predominant and population growth is either negligible (case (1)) or very slow (case (2)). As a consequence, despite μ returning to the initial non-inflammatory value at the end of the considered period (5 months), the ASM cell population size has not decreased to its original value. This feature results from the existence of different timescales in the model and accounts for the persistence of ASM remodelling in asthma beyond acute phases of inflammation (in agreement with a recent chronically-challenged mouse model of asthma [17]). Note that the theoretical model allows for the existence of a very slow decrease in ASM mass in the case of prolonged absence of hyperplastic stimulus (over a timescale of years, thus not apparent in Fig. 2d). Indeed, our model suggests that there is a dynamic balance between state-switching, proliferation and apoptosis in a population of ASM cells: $\lambda_{cp}/\lambda_{pc} \sim \lambda_a/\lambda_p$ (see S1.2 in Materials S1). Such a slow decay in ASM mass has been observed recently in an equine model of asthma (see Discussion and [18]).

Recurrent inflammatory episodes

Figure 3 shows examples of the different proliferation scenarios that can be encountered under a series of regular inflammatory events distributed over about one year, depending on the inflammation magnitude, frequency and resolution rate. When
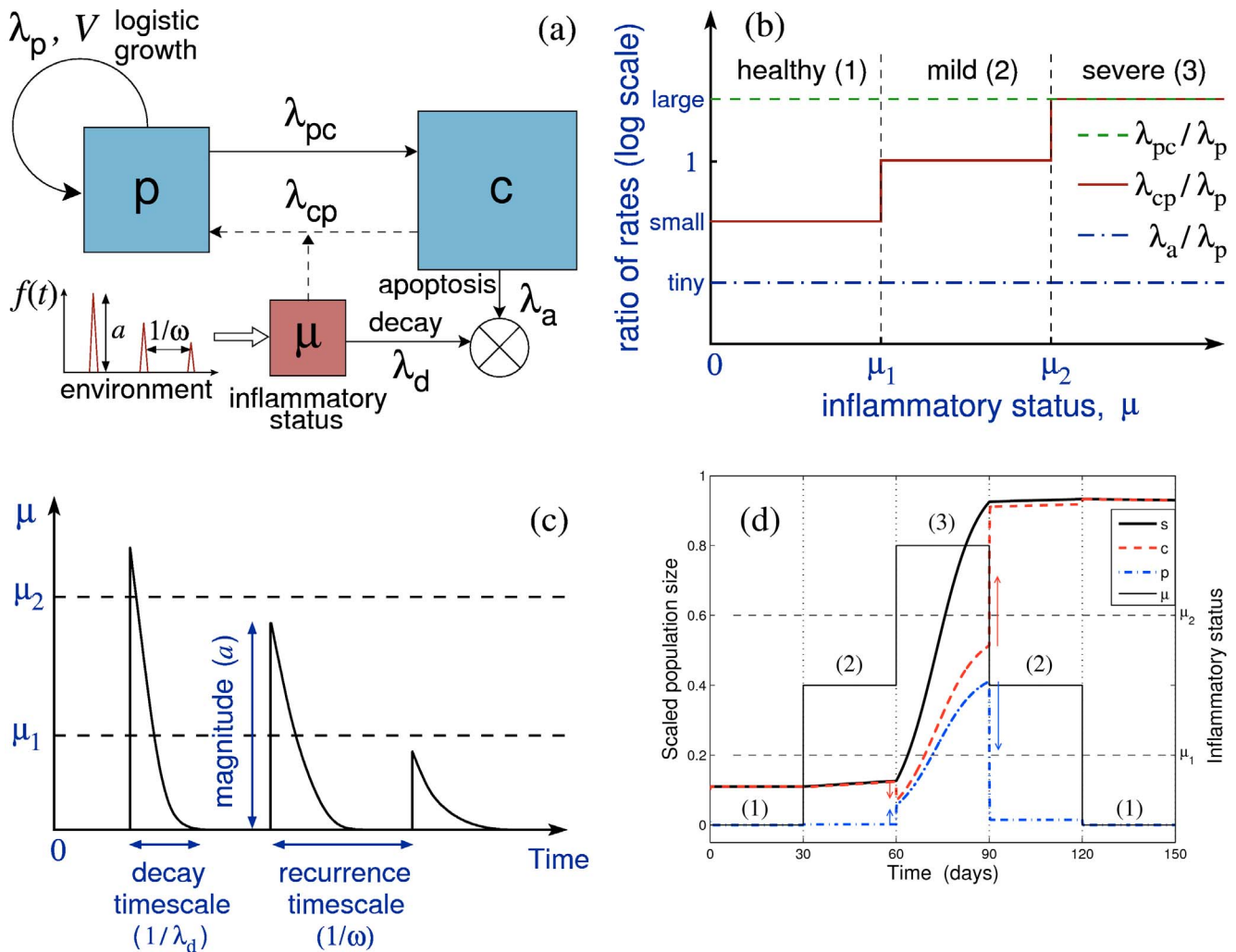
Figure 2. A schematic of the model design. (a) Schematic representation of the model with p being the amount of ASM cells in proliferating state, c the amount of non-proliferative cells and μ the inflammatory status; λ_p is the proliferation rate, λ_a is the apoptosis rate, λ_{cp} and λ_{pc} are the switching rates between non-proliferative and proliferative states, λ_d is the inflammation clearance rate, and $f(t)$ is a time-dependent external inflammatory stimulus. (b) Dependence of the model parameters on the inflammatory status μ (three levels of inflammation are characterised by the thresholds μ_1 and μ_2; see Table 1 for reference values). Rates are plotted on a logarithmic vertical scale. (c) An illustration of the inflammatory status dynamics induced by a series of environmental stimuli such as shown in (a), illustrating graphically the parameters λ_d, a, and ω. (d) A simulation of the ASM cell population response (p, blue dash-dotted; c, red dashed; $s = p+c$, thick black solid) to a stepwise variation in the inflammation status (thin solid); the arrows show the direction of change in the ASM subpopulations. Although the inflammatory status returns to its initial state at the end of the simulation, the total ASM cell population has irreversibly increased, showing thereby "effective" hysteresis. Only the time spent in "severe" regime ($\mu > \mu_2$) contributes to substantial growth (over weeks); however, the "moderate" regime ($\mu_1 < \mu < \mu_2$) can also give rise to substantial growth over a longer timescale (months). Note that the proportion of proliferative cells (blue dash-dotted) is significant only during the "severe inflammation" regime (3).
doi:10.1371/journal.pone.0090162.g002

the magnitude of inflammatory events is below the "severe" inflammation threshold μ_2 and the rate of resolution is high, there is no significant ASM mass increase (Fig. 3a); more severe inflammatory events, depending on their magnitude, lead to "moderate" (Fig. 3c) or "severe" (Fig. 3d) long-term ASM mass accumulation. Similarly, changing the frequency of the events from monthly (Fig. 3b) to semi-monthly (Fig. 3c), for the same magnitude and resolution rate, results in about two-fold ASM mass increase.

The outcome of the exacerbation events depends strongly on whether successive inflammatory events accumulate to increase the mean inflammatory status (Fig. 3e) or are independent (Fig. 3(a–d)). In particular, although the frequency and magnitude of inflammatory events are nearly identical in Figs 3(a) and 3(e),

the ASM mass remains unchanged in Fig. 3(a) while it increases substantially in Fig. 3(e), due to the slow inflammation resolution.

Figure 4 summarises the possible growth scenarios illustrated in Fig. 3(a–e). The relative fold-increase in ASM population size reached at the end of the observation period (300 days) is plotted as a function of the normalised inflammation resolution rate IR $= \lambda_d/\lambda_p$ (vertical axis), and (on the horizontal axis) the normalised inflammation magnitude a/μ_1 (Fig. 4a) or frequency ω/λ_p (Fig. 4b).

When the inflammation resolution is very slow (small IR $\ll 1$), the inflammatory status μ accumulates even if individual exacerbations are mild and infrequent, leading to severe increase in ASM mass for a wide range of magnitudes and frequencies (red zones in Fig. 4). Defining the boundaries between "healthy", "moderate" and "severe" outcomes in terms of the isolines for a

Table 1. Literature-based and estimated parameter values used in the ASM growth model.

Parameter	Value	Reference
ASM cell proliferation rate (λ_p) [*]	~1/3 days^{-1}	[5,7]
Remodelling time scale (T)	~100 days	[2]
Time-scale parameter ($\varepsilon = 1/(\lambda_p T)$)	0.02	
Relative $p \to c$ switching rate (λ_{pc}/λ_p)	50 ($\sim \varepsilon^{-1}$)	
Relative $c \to p$ switching rate (λ_{cp}/λ_p)	0.016 ($\sim \varepsilon$) for $\mu < \mu_1$,	
	0.8 (~ 1) for $\mu_1 < \mu < \mu_2$,	
	40 ($\sim \varepsilon^{-1}$) for $\mu > \mu_2$	
Relative ASM apoptosis rate (λ_a/λ_p)	4×10^{-4} ($\sim \varepsilon^2$)	
Relative severe inflammatory threshold (μ_2/μ_1)	2.5	
Relative inflammatory stimulus magnitude (a/μ_1)	0.1–10	
Relative frequency of inflammatory events (ω/λ_p)	0.1–1 (monthly – weekly)	
Inflammation resolution rate IR $= \lambda_d/\lambda_p$	0.1–10	

([*] indicates the values estimated from *in vitro* experiments.)

given long-term fold-increase in ASM mass (the two thick solid lines in Fig. 4(a), corresponding respectively to 2- and 8-fold increase), we see that the chance of an individual being in the "moderate" ASM growth regime, as either the exacerbation magnitude or frequency are increased, drops considerably when the inflammation resolution is slow (IR <1), indicating the possibility of a catastrophic shift straight from the "healthy" to the "severe remodelling" scenario when the inflammation resolution is not fast enough.

For very rapid inflammation resolution (high IR >>1), when the individual inflammatory episodes are almost independent of each other, the long-term ASM mass accumulation is determined solely by the total time spent with inflammatory status above the "severe" inflammation threshold ($\mu \geq \mu_2$). Our analysis (see S1.2 in Materials S1) shows that this time is linearly proportional to the exacerbation frequency ω, but the dependence on the relative inflammatory event magnitude a/μ_2 is nonlinear. Hence, the isolines of constant ASM growth are expected to obey IR $\sim (\omega/\lambda_p)$ $\log(a/\mu_2)$ (white dashed lines in Fig. 4; see also S1.2 in Materials S1). This theoretical prediction agrees well with the computed growth isolines (thick black lines in Fig. 4) for IR >1. The model therefore suggests an integral *inflammation severity* (IS) index

$$\frac{(\text{exposure frequency}) \times \log(\text{exposure magnitude})}{(\text{inflammation resolution speed})}$$

(where exposure magnitude is measured relative to the threshold), which has the potential to be used as a predictor of long-term ASM remodelling in the case of moderate-to-fast inflammation resolution. In other words, given the time series of a biomarker of inflammation for a cohort of patients, the model indicates that the IS index computed from these series could correlate with the degree of ASM accumulation in this group.

Individual history effects in ASM growth

For slow recovery from inflammation (IR <1), substantial ASM mass growth can occur even if the inflammatory magnitude lies below the "severe" inflammation threshold ($a < \mu_2$; see e.g. Fig. 3e), in contrast to the fast IR case which requires $a > \mu_2$ for substantial growth. Therefore, the individual history of inflammatory, pro-remodelling events can have a very strong impact on the degree of

long-term ASM hyperplasia when successive events can accumulate.

Figure 5 illustrates the importance of history in determining the outcome of a series of inflammatory episodes, when the inflammation resolution is slow. For given inflammation magnitude, frequency and resolution rate, the amount of ASM growth elicited by an inflammatory event depends crucially on the timing of the previous inflammatory events. For example, for regular episodes at a frequency of about once a fortnight (Fig. 5d) and small inflammation magnitude, the inflammatory status lies well within the "moderate inflammation" zone after about 40 days, leading to a "moderate" (less than 3-fold) long-term increase in ASM mass (Fig. 5a). However, when the events occur irregularly (Fig. 5(e,f)) with the same average characteristics as in Fig. 5(d), the individual long-term outcome is much more diverse (Fig. 5(b,c)), due to the possibility of accumulated inflammatory events or prolonged periods of remission.

In order to demonstrate the impact of dangerously frequent exacerbations, Figure 5(g) shows the distribution (histogram) of $N = 1000$ possible outcomes in a given individual at the end of an observation period of 300 days (for a series of random events exemplified in Fig. 5(e,f)). The distribution is bimodal (i.e. has two peaks), with one mode being close to the nearly "healthy" state reached in the absence of randomness (Fig. 5(a,d)), and the other mode corresponding to severe increase in ASM mass (Fig. 5(c,f)). Figure 5(h) shows that an increase of only 25% in the inflammation resolution rate IR can substantially push the mean of the distribution toward the "healthy" mode. This emphasises the importance of individual inflammatory history for prognosis and management of ASM hyperplasia.

We further survey the effect of variability in the timing of acute inflammatory stimuli in Figure 6, which is the analogue of Fig. 4(a) for the case of randomly occurring exacerbation events, and is plotted for a whole range of inflammation resolution rates and magnitudes. Each point in Fig. 6(a) represents the mean long-term fold-increase in ASM mass (at the end of 300 days) for given inflammation characteristics, while each point in Fig. 6(b) represents the variability of the outcome (quantified as the ratio of standard deviation to the mean). Some representative distributions of outcomes are shown in Fig. 6(i–iv).

Figure 6(a) indicates that, at slow resolution rates, the "moderate remodelling" transition zone is larger for random
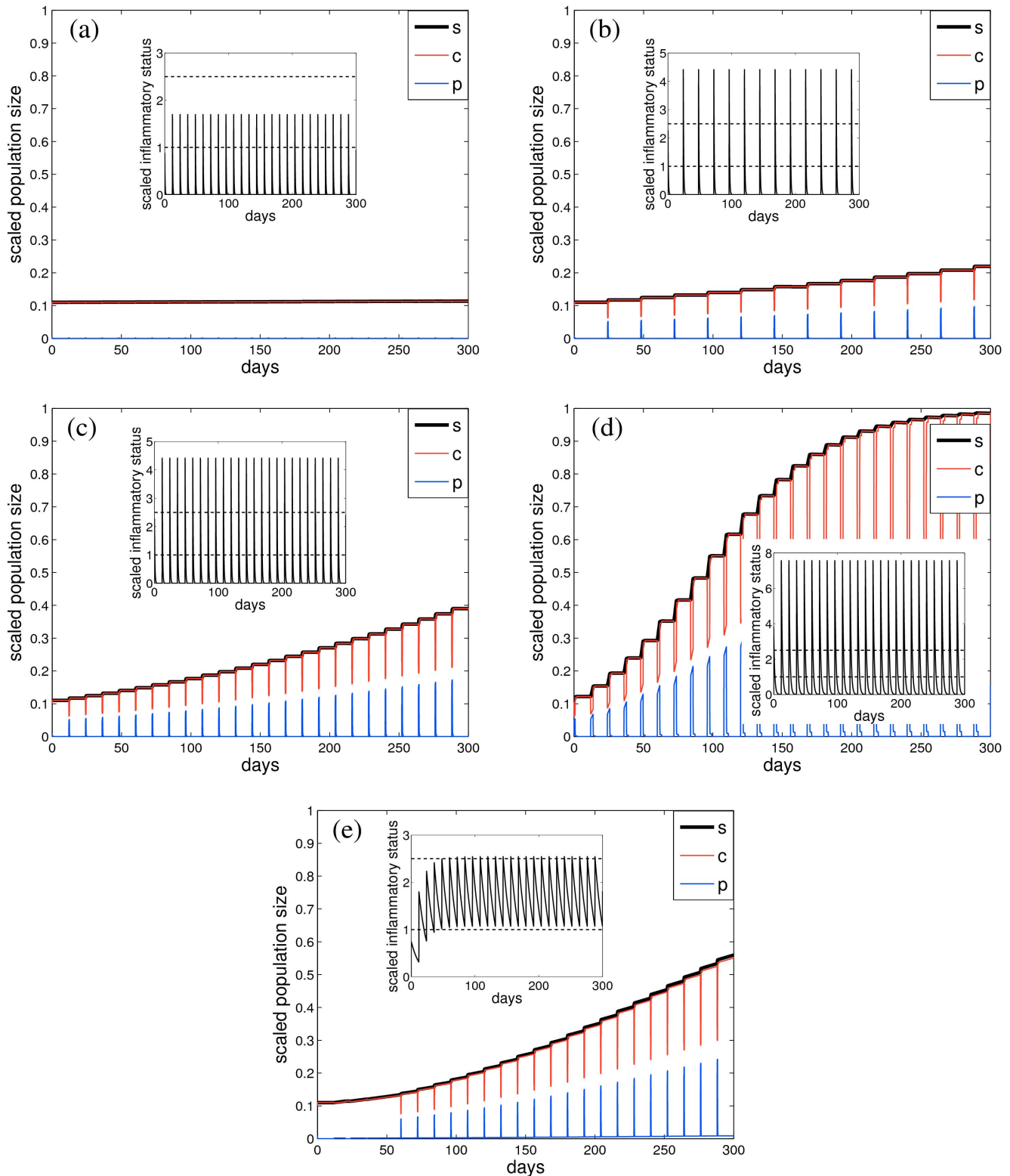
Figure 3. Representative ASM cell population growth dynamics over a period of 300 days, starting from a ''healthy'' state ($c = 0.1$, $p = 0.01$), for different values of normalised inflammation magnitude a/μ_1, frequency ω/λ_p and inflammation resolution rate λ_d/λ_p: $a/\mu_1 = \{2\ (a),\ 5\ (b,c),\ 8\ (d),\ 1.5\ (e)\}$, $\omega/\lambda_p = \{0.25\ (a,c-e),\ 0.125\ (b)\}$ and $\lambda_d/\lambda_p = \{7\ (a),\ 5\ (b,c),\ 2\ (d),\ 0.22\ (e)\}$. (a,b) show no substantial ASM accumulation, (c,e) show ''moderate'' and (d) ''severe'' ASM hyperplasia. The amount of c-cells is depicted by the red line, p-cells (blue) and total population size $s = p + c$ (thick black). Insets plot the corresponding inflammatory status μ (solid black) and the inflammation level thresholds (horizontal dashed lines).

doi:10.1371/journal.pone.0090162.g003
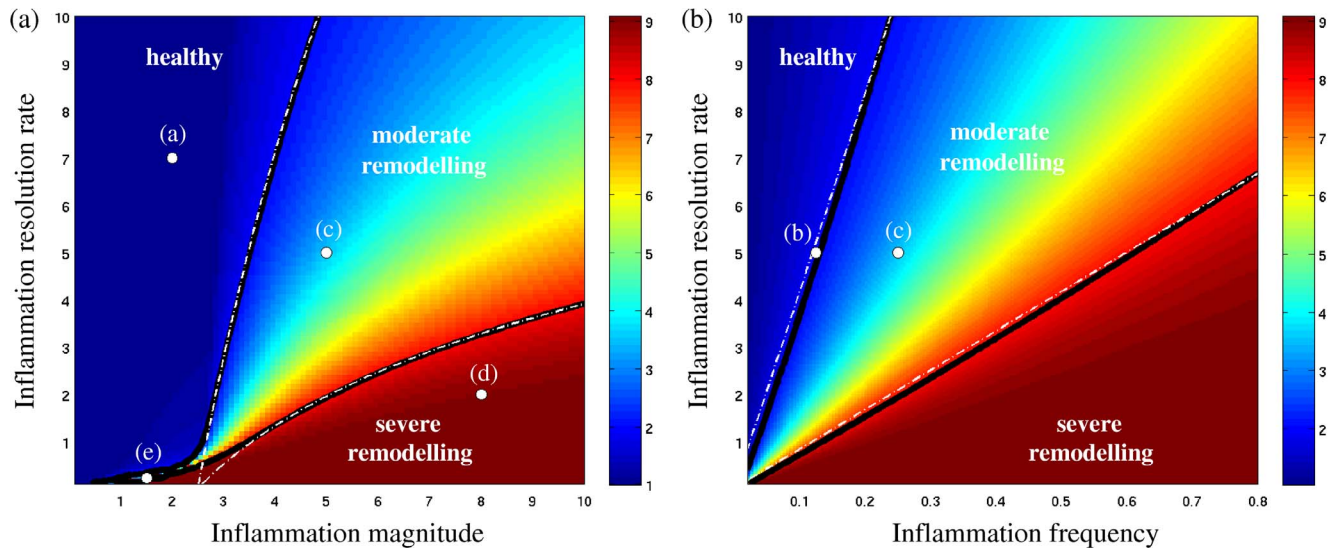
Figure 4. Survey of ASM growth scenarios, showing fold-increase in ASM population size after 300 days (colour scale) as a function of the inflammation resolution rate IR = λ_d/λ_p and (a) inflammation magnitude a/μ_1 (for fixed frequency ω/λ_p = 0.25) or (b) inflammation frequency ω/λ_p (for fixed magnitude a/μ_1 = 5). White dots indicate the growth regimes shown in Fig. 2. Solid black lines are the computed isolines of the 2- and 8-fold ASM growth, which agree with the theoretically predicted dependence $\lambda_d \sim \omega \log a/\mu_2$ (dashed white lines; see Materials S1).
doi:10.1371/journal.pone.0090162.g004

inflammatory episodes (Fig. 6a) than for regular episodes (Fig. 4a). Figure 6(b) shows that the variability of "healthy" and "severe remodelling" outcomes (blue zone in Fig. 6(b)) is very low; uncertainty is mainly concentrated in the "moderate remodelling" zone, and rapidly diminishes as resolution speed increases (Fig. 6b).

The high uncertainty region (yellow-to-red, Fig. 6b) is characterised by a very wide distribution of outcomes, even though some of these distributions (e.g. Fig. 6(iv)) have relatively low mean values of long-term ASM growth. These are therefore as undesirable as high-mean distributions (e.g. Fig. 6(i)) due to a high risk of ending up with "severe" remodelling in the long term.

Discussion

In this work, we have proposed a simple model of inflammation-induced ASM hyperplasia, an important aspect of airway remodelling in asthma. The model assumes that ASM cells can be in one of two states: 'proliferative' (also accounting for the recruitment and differentiation of fibroblasts and myofibroblasts by inflammatory mediators [19]) or 'non-proliferative'. Although the former is usually associated with a synthetic activity, and the latter with a contractile activity, we avoided using this additional terminology here since the synthetic and contractile functions of ASM cells may not be mutually exclusive [20]. Bidirectional switching between the two states is allowed (as observed *in vitro* in both human ASM cells in culture and in human tracheal smooth muscle strips [13,21]), and it is assumed that the level of the inflammatory status μ controls the rate of switching between the two ASM states via the existence of two sensitivity thresholds (Fig. 2b). With the aid of mathematical techniques (see Materials S1), we have shown that this leads to the existence of three corresponding ASM growth regimes (Fig. 2d) and three qualitatively different remodelling outcomes (Figs 4 and 6), matching the classification commonly used in clinical practice [6,22].

The existence of different timescales in the model accounts for several important features of asthma:

i. the persistence of airway remodelling despite the resolution of acute inflammation [1,17], and the correlation of ASM mass with asthma severity rather than with asthma duration [23];

ii. the presence of airway remodelling and abnormal lung function very early in the history of asthma [24];

iii. the very slow decline (of the order of years) in ASM mass in the continued absence of hyperplastic stimuli [18].

Feature (i) can be directly related to Fig. 2(d); feature (ii) can be explained by μ having crossed the severe inflammation threshold, and remained above it a substantial amount of time, early in the disease history; feature (iii) is consistent with the non-negligible role played by apoptosis when the inflammatory status is kept in the healthy range (Fig. 2b) for a sufficiently long time (longer than that considered in Fig. 2(d); see also S1.2 in Materials S1).

Cumulative effects of individual inflammatory history at slow resolution rate

Assuming that inflammatory events are characterised by transient increases in the inflammatory status μ (Fig. 2c), our model predicts that long-term ASM growth is essentially controlled by three parameters: the inflammation resolution speed (IR), the inflammation magnitude (relative to the two sensitivity thresholds μ_1 and μ_2) and the frequency of inflammatory episodes. The severity and frequency of the inflammatory episodes could be targeted to ensure that an asthmatic individual does not fall into the dangerous "severe remodelling" zone (red in Fig. 4). However, our model indicates that faster inflammation resolution could offer a better protection against severe ASM remodelling by increasing the probability of "healthy state" or "moderate" growth (see Figs 4a and 6a).

In addition, irregularity of the occurrence of inflammatory episodes, together with the existence of sensitivity thresholds, lead to a large variability of growth scenarios (see "moderate remodelling" region in Figs 5(b,c) and 6). Thus, one should take into account not only the expected outcome but also the degree of
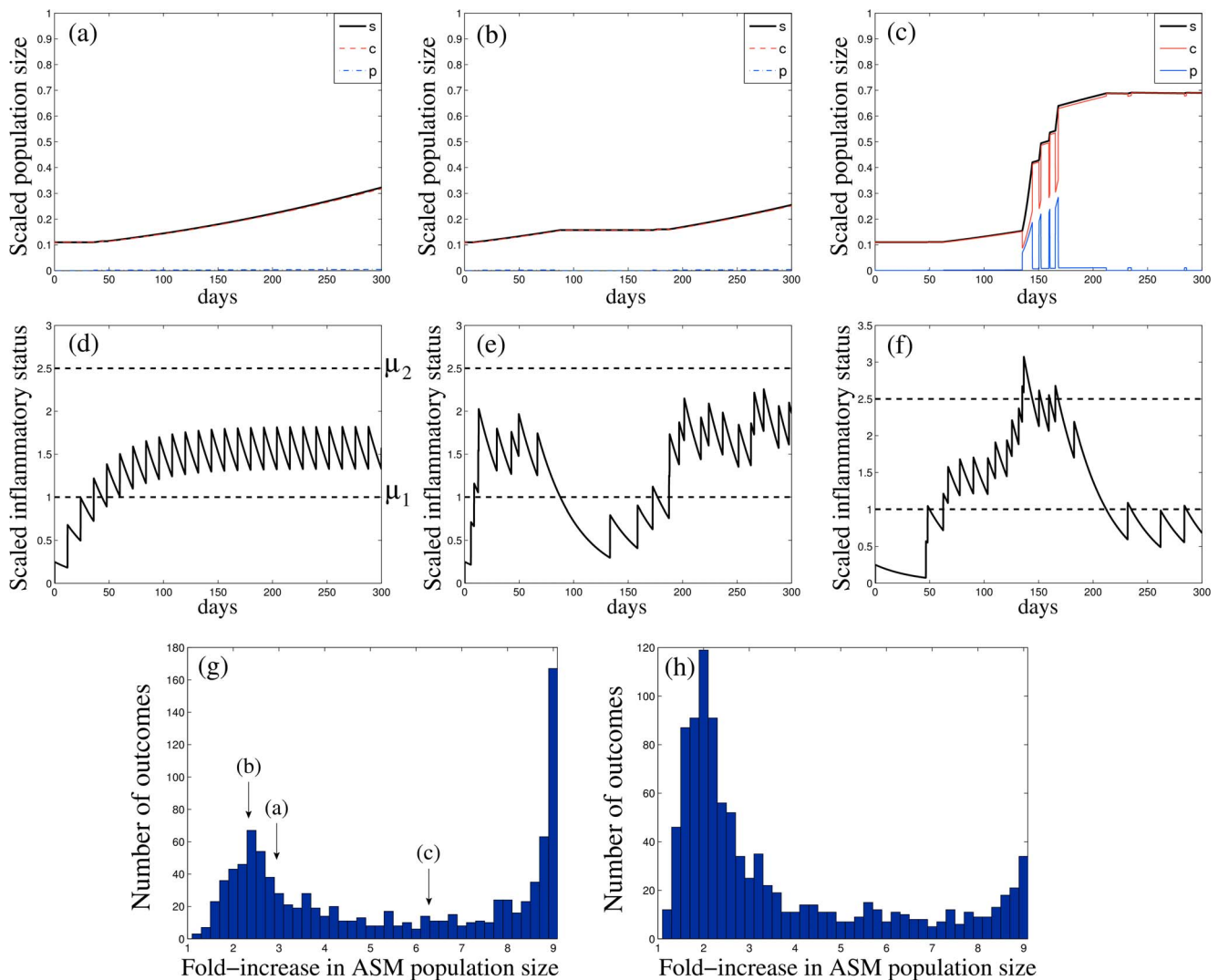
Figure 5. The role of individual inflammation history in the case of slow inflammation resolution (IR ≪1). (a–c) ASM population size dynamics (c-cells, red; p-cells, blue; total population s, black) and (d–f) the corresponding inflammatory status evolution (μ, solid black; inflammatory thresholds μ₁ and μ₂, dashed), characterized by the same inflammation resolution rate, magnitude and average stimulus frequency (λ_d/λ_p = 0.08, a/μ_1 = 0.5, ω/λ_p = 0.25). (d) Regular series of inflammatory events; (e–f) two realisations of a series of inflammatory events at random times for the same mean frequency (about once a fortnight) as in (d). (g) Distribution of fold-increase in ASM mass after 300 days for a random sequence of inflammatory events with the same characteristics as in panels (b, c); arrows indicate the fold-increase corresponding to (a–c). (h) The distribution of outcomes with an increase of 25% in the inflammation resolution rate (λ_d/λ_p = 0.1). (The outcome histograms (g,h) are computed for N = 1000 instances).
doi:10.1371/journal.pone.0090162.g005

uncertainty when deciding on the optimal low-risk treatment strategy (see arrows in Fig. 6a). That means it would be desirable to avoid high outcome variability (Fig. 6b) when navigating towards the "healthy" state by varying the inflammation resolution speed, magnitude or frequency. (Note that another possibility would be to modify the landscape of outcomes itself by elevating the inflammation sensitivity threshold μ₂, thereby "moving the mountain rather than the man"). These results emphasise the importance of individual inflammatory history for prognosis and management of ASM hyperplasia in individuals where slow resolution of inflammation is suspected.

A recent study of a horse model of asthma [18] supports these results by comparing the effect of inflammation resolution speed (modulated by corticosteroids) and the role of frequency and severity of environmental stimuli (by avoidance of antigen exposure). Leclere and colleagues have shown that treatment with

corticosteroids gives more rapid (compared to pure antigen avoidance) effects on lung function and ASM remodelling [18], which agrees with our model's prediction of the higher importance of rapid inflammation resolution over stimulus magnitude (see Fig. 6a). This prediction is also supported by the acceleration of ASM mass decline by corticosteroids observed in human peripheral airways after a 6-week treatment [25]. Indeed, the ASM cell population can decrease (very slowly) only when μ is below the mild inflammation threshold (Fig. 2b). The larger the inflammation resolution speed, the sooner this long-term recovery regime can be reached.

Long-term ASM mass accumulation at moderate-to-fast resolution rate

Faster resolution of inflammation decouples individual pro-inflammatory events and thus diminishes the effect of inflamma-
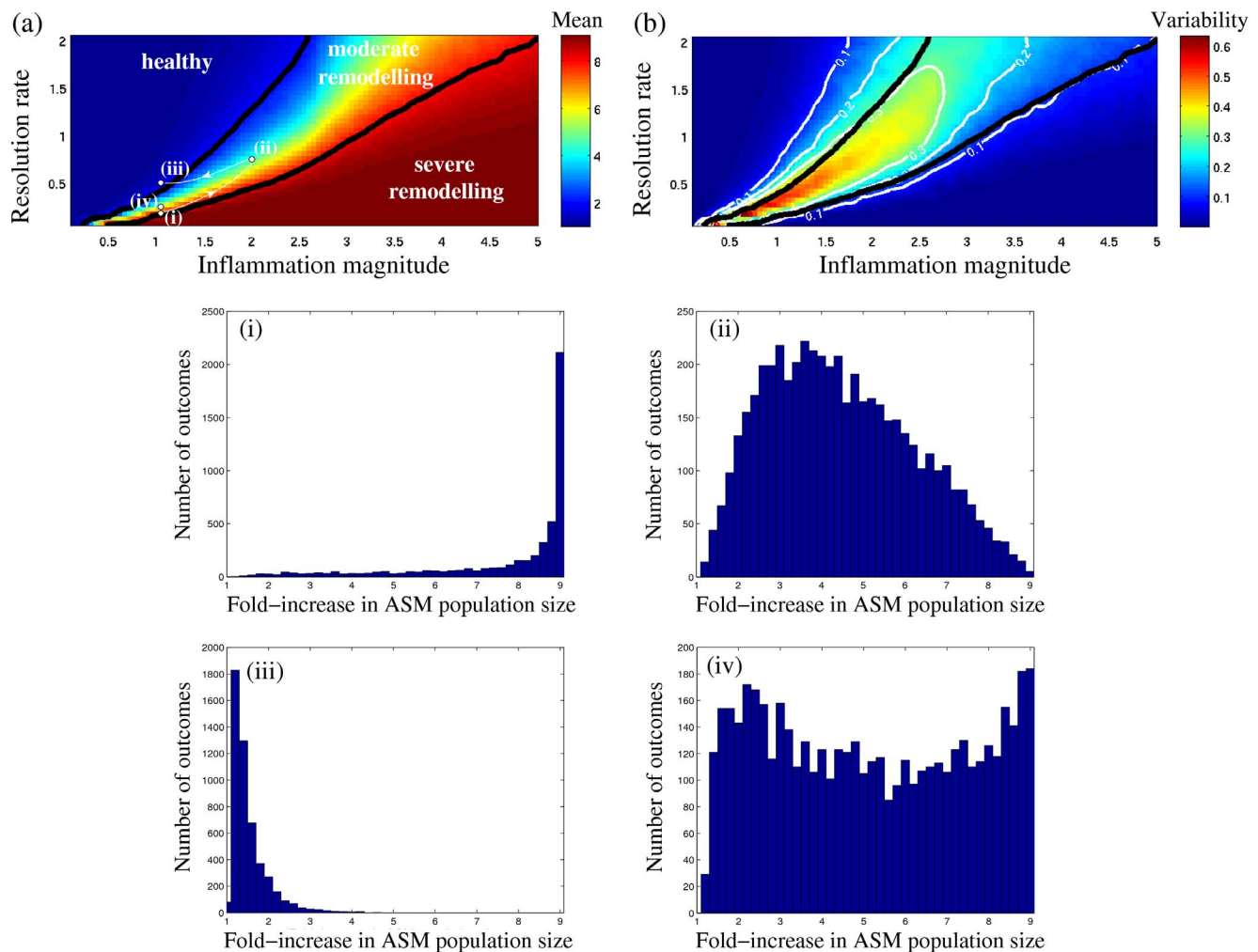
Figure 6. Survey of stochastic ASM growth scenarios in the region of low-to-moderate inflammation resolution rate. (a) Mean fold-increase in the ASM population size at 300 days (colour scale) as a function of inflammation resolution rate IR $= \lambda_d/\lambda_p$ and inflammation magnitude a/μ_1 (*cf*. Fig. 3a). (b) Corresponding uncertainty (colours) quantified as the ratio of SD to the mean; white lines indicate the uncertainty isolines. (Solid black lines in (a,b) show 2- and 8-fold increase in mean; computed for a sample size of $N = 500$ random realisations). The parameter dependence of outcome distributions ($N = 5000$) are illustrated in (i–iv), indicated by white dots in (a). (Note the variation in vertical scales between panels (i, iii) and (ii, iv)). The quickest transition from (i) to (iii) crosses the high uncertainty region ((iv), red in panel (b)), while a trajectory that bypasses it (white line in (a)) protects against "severe" remodelling outcomes.
doi:10.1371/journal.pone.0090162.g006

tion history in ASM growth. Although this seems to provide greater control over ASM population growth, a mild-to-moderate accumulation of ASM mass over the long term can still occur, provided the magnitude of the exacerbation is above the second threshold μ_2. The model predicts that long-term ASM mass accumulation is proportional to exacerbation frequency but depends less strongly on exacerbation magnitude (see the growth isolines in Fig. 4). The frequency of the pro-inflammatory events could therefore be considered a secondary target, after ensuring rapid resolution of inflammation. The importance of antigen exposure frequency in the degree of airway remodelling has been also confirmed in animal models [26].

Given that resolution of exacerbations can be affected by current therapies [27] and that clinical factors associated with frequent exacerbations are well recognised [28], mechanism-derived links between these factors and exacerbations could be targeted in future studies to prevent airway remodelling.

Model limitations and further development

While accounting for the key features of ASM growth, the proposed model neglects many potentially important factors, such as the detailed pathways governing ASM hyperplasia. However, the kinetic parameters for these pathways remain largely unknown. The generality of our model is also a strength, in that its predictions do not depend on the precise nature of the signalling events (leading to the increase in the "inflammatory status") but only on their dynamical features (magnitude, frequency, resolution speed). In particular, the model is compatible with bronchocon-striction acting as a trigger of airway remodelling [15,16].

We have not included mechanical interaction of the cells between each other and with the extracellular matrix that could affect the growth and apoptosis rates as well as the total capacity V of an airway wall. Our model additionally neglects the spatially heterogeneous and anisotropic growth observed in micrographs and cell hypertrophy. Therefore, the predictions of this ASM growth model are qualitative rather than quantitative.

Extra care should also be taken when interpreting the results of the model in terms of its impact on respiratory lung function. Relative increase in the lumen-narrowing contractile force of an airway wall due to a larger ASM mass could be balanced by a simultaneous increase in the wall stiffness, which may have a constriction-limiting effect [29]. Future models should therefore focus on coupling the mechanics of an airway wall and the ASM population dynamics [29–31].

Further experiments to test the model prediction of the role of inflammation resolution rate in co-cultures of inflammatory and ASM cells or in animal models (such as the studies of Garn and co-workers [17,32]) would be desirable. It would also be of interest to use the model results (in particular, the inflammation severity index) for a detailed statistical analysis of inflammatory status from a time series of inflammatory biomarkers (such as eosinophil counts in sputum or exhaled nitric oxide concentration) and their relation to ASM mass in bronchial biopsies. To our knowledge such longitudinal studies have not yet been performed, due to the difficulties in carrying out repetitive airway biopsies in humans.

Conclusions

We have developed and analysed a theoretical model of ASM mass accumulation driven by a series of exacerbation events. Our model highlights the importance of the resolution speed of inflammation in long-term management of asthma. It exposes the possibility of false security of strict antigen avoidance or reduced sensitivity to inflammatory stimuli. A few accidental exposures or acute exacerbations at impaired resolution can lead to the accumulation of inflammatory status and hence relatively rapid ASM remodelling.

A more robust anti-remodelling strategy could lie in ensuring the rapid clearance of growth or recruitment factors during the post-exacerbation period, thereby protecting against dangerous build-up of these factors, latent ASM mass increase and reducing the risk of severe remodelling.

Supporting Information

Material S1 Supplementary information on the design and solution techniques for the mathematical model. (PDF)

Acknowledgments

The authors would like to thank all the organisers and participants of the 2011 Mathematics-in-Medicine Study Group (MMSG), in particular, Michelle Baker (University of Nottingham), Dr Anthony M. Holmes (NC3Rs), Dr Joel M. Phillips (University College London) and Thomas J. Snowden (University of Reading) for many discussions that stimulated this study.

Author Contributions

Conceived and designed the experiments: ILC LACC HC BSB OEJ IPH CKB SRJ. Performed the experiments: ILC LACC LSK JEH. Analyzed the data: ILC. Contributed reagents/materials/analysis tools: ILC LACC LSK JEH OEJ. Wrote the paper: ILC HC BSB OEJ CKB SRJ.

References

1. Kariyawasam HH, Aizen M, Barkans J, Robinson DS, Kay AB (2007) Remodeling and airway hyperresponsiveness but not cellular inflammation persist after allergen challenge in asthma. Am J Respir Crit Care Med 175: 896–904.
2. Mauad T, Bel EH, Sterk PJ (2007) Asthma therapy and airway remodeling. J Allergy Clin Immunol 120: 997–1009.
3. Bentley JK, Hershenson MB (2008) Airway smooth muscle growth in asthma: proliferation, hypertrophy, and migration. Proc Am Thorac Soc 5: 89–96.
4. James AL, Elliot JG, Jones RL, Carroll ML, Mauad T, et al. (2012) Airway smooth muscle hypertrophy and hyperplasia in asthma. Am J Respir Crit Care Med 185: 1058–1064.
5. Johnson PRA, Roth M, Tamm M, Hughes M, Ge Q, et al. (2001) Airway smooth muscle cell proliferation is increased in asthma. Am J Respir Crit Care Med 164: 474–477.
6. Hirst SJ, Martin JG, Bonacci JV, Chan V, Fixman ED, et al. (2004) Proliferative aspects of airway smooth muscle. J Allergy Clin Immunol 114: S2–S17.
7. Kaur D, Hollins F, Saunders R, Woodman L, Sutcliffe A, et al. (2010) Airway smooth muscle proliferation and survival is not modulated by mast cells. Clin Exp Allergy 40: 279–288.
8. Brightling CE, Bradding P, Symon FA, Holgate ST, Wardlaw AJ, et al. (2002) Mast-cell infiltration of airway smooth muscle in asthma. N Engl J Med 346: 1699–1705.
9. Baker M, Billington C, Chapman LAC, Chernyavsky IL, Croisier H, et al. (2011) Mathematical modelling of airway smooth muscle cell proliferation and apoptosis in asthma. Reading: Mathematics-in-Medicine Study Group Report. 31 p.
10. Holmes AM, Solari R, Holgate ST (2011) Animal models of asthma: value, limitations and opportunities for alternative approaches. Drug Discov Today 16: 659–670.
11. Contoli M, Bousquet J, Fabbri LM, Magnussen H, Rabe KF, et al. (2010) The small airways and distal lung compartment in asthma and COPD: a time for reappraisal. Allergy 65: 141–151.
12. Halayko AJ, Camoretti-Mercado B, Forsythe SM, Vieira JE, Mitchell RW, et al. (1999) Divergent differentiation paths in airway smooth muscle culture: induction of functionally contractile myocytes. Am J Physiol - Lung Cell Mol Physiol 276: L197–L206.
13. Dekkers BG, Bos IST, Zaagsma J, Meurs H (2012) Functional consequences of human airway smooth muscle phenotype plasticity. Br J Pharmacol 166: 359–367.
14. Markwick LJ, Clements D, Roberts ME, Ceresa CC, Knox AJ, et al. (2012) CCR3 induced-p42/44 MAPK activation protects against staurosporine induced-DNA fragmentation but not apoptosis in airway smooth muscle cells. Clin Exp Allergy 42: 1040–1050.
15. Grainge CL, Lau LCK, Ward JA, Dulay V, Lahiff G, et al. (2011) Effect of bronchoconstriction on airway remodeling in asthma. N Engl J Med 364: 2006–15.
16. Tatler AL, John AE, Jolly L, Habgood A, Porte J, et al. (2011) Integrin αvβ5-mediated TGF-β activation by airway smooth muscle cells in asthma. J Immunol 187: 6094–107.
17. Alrifai M, Marsh LM, Dicke T, Kılıç A, Conrad ML, et al. (2014) Compartmental and temporal dynamics of chronic inflammation and airway remodelling in a chronic asthma mouse model. PLoS ONE 9: e85839.
18. Leclere M, Lavoie-Lamoureux A, Joubert P, Relave F, Setlakwe EL, et al. (2012) Corticosteroids and antigen avoidance decrease airway smooth muscle mass in an equine asthma model. Am J Respir Cell Mol Biol 47: 589–596.
19. Alkhouri H, Hollins F, Moir LM, Brightling CE, Armour CL, et al. (2011) Human lung mast cells modulate the functions of airway smooth muscle cells in asthma. Allergy 66: 1231–1241.
20. Hirota JA, Nguyen TT, Schaafsma D, Sharma P, Tran T (2009) Airway smooth muscle in asthma: Phenotype plasticity and function. Pulm Pharmacol Ther 22: 370–378.
21. Hirst SJ, Twort CHC, Lee TH (2000) Differential effects of extracellular matrix proteins on human airway smooth muscle cell proliferation and phenotype. Am J Respir Cell Mol Biol 23: 335–344.
22. Louis R, Sele J, Henket M, Cataldo D, Bettiol J, et al. (2002) Sputum eosinophil count in a large population of patients with mild to moderate steroid-naive asthma: distribution and relationship with methacholine bronchial hyperresponsiveness. Allergy 57: 907–912.
23. James AL, Bai TR, Mauad T, Abramson MJ, Dolhnikoff M, et al. (2009) Airway smooth muscle thickness in asthma is related to severity but not duration of asthma. Eur Respir J 34: 1040–5.
24. Payne DNR, Rogers AV, Adelroth E, Bandi V, Guntupalli KK, et al. (2003) Early thickening of the reticular basement membrane in children with difficult asthma. Am J Respir Crit Care Med 167: 78–82.
25. Bergeron C, Hauber HP, Gotfried M, Newman K, Dhanda R, et al. (2005) Evidence of remodeling in peripheral airways of patients with mild to moderate asthma: effect of hydrofluoroalkane-flunisolide. J Allergy Clin Immunol 116: 983–9.
26. Allen JE, Bischof RJ, Sucie Chang H-Y, Hirota JA, Hirst SJ, et al. (2009) Animal models of airway inflammation and airway smooth muscle remodelling in asthma. Pulm Pharmacol Ther 22: 455–465.
27. Tattersfield AE, Postma DS, Barnes PJ, Svensson K, Bauer C-A, et al. (1999) Exacerbations of asthma. Am J Respir Crit Care Med 160: 594–599.
28. ten Brinke A, Sterk PJ, Masclee AAM, Spinhoven P, Schmidt JT, et al. (2005) Risk factors of frequent exacerbations in difficult-to-treat asthma. Eur Respir J 26: 812–818.

29. Brook BS, Peel SE, Hall IP, Politi AZ, Sneyd J, et al. (2010) A biomechanical model of agonist-initiated contraction in the asthmatic airway. Respir Physiol Neurobiol 170: 44–58.

30. Byrne H, Preziosi L (2003) Modelling solid tumour growth using the theory of mixtures. Math Med Biol 20: 341–366.

31. Moulton DE, Goriely A (2011) Possible role of differential growth in airway wall remodeling in asthma. J Appl Physiol 110: 1003–1012.

32. Wegmann M, Fehrenbach H, Fehrenbach A, Held T, Schramm C, et al. (2005) Involvement of distal airways in a chronic model of experimental asthma. Clin Exp Allergy 35: 1263–1274.

Supplementary Material

The role of inflammation resolution speed in airway smooth muscle mass accumulation in asthma: insight from a theoretical model

I.L. Chernyavsky[1,*], H. Croisier[1], L.A.C. Chapman[2], L.S. Kimpton[2], J.E. Hiorns[1],
B.S. Brook[1], O.E. Jensen[3], C.K. Billington[4], I.P. Hall[4], S.R. Johnson[4]

S1 Supplementary Methods

This section gives additional technical details about the design and solution techniques for the model.

S1.1 Model Assumptions and Formulation

Consider the following system of ordinary differential equations, describing the dynamics of two subpopulations of ASM cells defined in Fig. 2(a,b):

$$\dot{p} = \lambda_p\, p \left(1 - \frac{p + c}{V} \right) - \lambda_{pc}\, p + \lambda_{cp}\, c \,, \tag{S1a}$$

$$\dot{c} = \lambda_{pc}\, p - (\lambda_{cp} + \lambda_a)\, c \,, \tag{S1b}$$

where p and c are the size of p- and c-subpopulations respectively (e.g. measured in number of cells per cross-sectional airway wall area), a dot over a variable represents its rate of change (a time derivative), λ_p is the proliferation rate, λ_a is the apoptosis rate, and λ_{pc}, λ_{cp} are the switching rates, and V is the total capacity (maximal population size, measured in the same units as p and c). The system (S1) is subject to the initial conditions $p|_{t=0} = p_0$ and $c|_{t=0} = c_0$. The total size of the ASM population is thus given by

$$s = p + c \,. \tag{S2}$$

We incorporate the effect of short-term inflammatory events by assuming that the switching rate λ_{cp} can change according to the inflammatory status μ which, for instance, could represent airway eosinophil cell count in sputum per unit volume. The dynamics of μ is described by the following equation:

$$\dot{\mu} = -\lambda_d\, \mu + a\, f(t;\omega) \,, \quad f(t;\omega) = \sum_i \delta(t - t_i), \tag{S3}$$

---

[*] Author for correspondence (Igor.Chernyavsky@nottingham.ac.uk).
[1] School of Mathematical Sciences, University of Nottingham
[2] Mathematical Institute, University of Oxford
[3] School of Mathematics, University of Manchester
[4] Department of Therapeutics and Molecular Medicine, University of Nottingham

where δ denotes Dirac's δ-function, t_i is the time of an acute inflammatory event, λ_d is the decay rate of the inflammatory factor, a is the magnitude of a single acute inflammatory event, and $\omega = 1/\mathbb{E}[t_{i+1} - t_i]$ is the mean event frequency.

All parameter ratios are expressed in terms of a small parameter $\varepsilon \equiv 1/(\lambda_p T)$, which is defined as the ratio of the proliferation timescale $1/\lambda_p$ to the remodelling timescale T; Table 1 gives the scalings of the corresponding ratios of rates used in the model. It should also be noted that the choice of the relative orders of magnitude for the rates (Fig. 2b) is not unique; however, a global rescaling of all the parameters by a power of ε does not affect our main conclusions. Also, similar results could be obtained by assuming that λ_{pc}, rather than λ_{cp}, or their ratio, are functions of μ.

S1.2 Solution Techniques

We use a combination of linear stability analysis, two-time-scale asymptotics and numerical simulation to characterise qualitatively the dynamics of a population of ASM cells. Direct numerical simulation of (S1)–(S3) is performed with `Matlab ode45` Runge-Kutta solver at the relative tolerance of 10^{-6}, where individual inflammatory events in (S3) are approximated as a series of Gaussian "peaks" $f(t) \approx \sum_i \exp\{-\lambda_p^2 (t - t_i)^2/(2\sigma^2)\}/\sqrt{2\pi\sigma^2}$ for $\sigma = 0.01 \ll \lambda_p/\omega$.

ASM growth dynamics

For the given assumptions, equations (S1) lead to three distinct asymptotic growth regimes for a population of ASM cells.

The first regime (case (1) in Fig. 2(b,d)) is characterised by an approximately constant c-subpopulation and negligible p-subpopulation when the balance between the state-switching, proliferation and apoptosis

$$\frac{\lambda_{cp}}{\lambda_{pc}} \sim \frac{\lambda_a}{\lambda_p} \tag{S4}$$

is satisfied; in the second growth regime (case (2) in Fig. 2(b,d)), the c-subpopulation of ASM cells exhibits a slow logistic growth, which is significant only in the long term (i.e. months to years), while the p-subpopulation remains small; in the third regime (case (3) in Fig. 2(b,d)), the ASM cell population splits into the c- and p-subpopulations of comparable size that grow logistically in relatively short time-scales (i.e. weeks to months).

Considering the dynamics of the inflammatory status μ for the moderate-to-large speed of inflammation resolution (IR $\equiv \lambda_d/\lambda_p \gtrsim 1$), an approximate solution to (S3) takes the form of a series of independent 'spikes' (Fig. S1):

$$\mu(t) \approx a \sum_{i=0}^{n} \mathrm{e}^{-\mathrm{IR}\,\lambda_p\,(t - t_i)}, \tag{S5}$$

where $n \equiv \lfloor \omega\, t \rfloor$ ($\lfloor x \rfloor$ denotes the integer part of x).

Since the time spent by an ASM cell population above the "severe" inflammation sensitivity threshold μ_2 has the greatest impact on the net population growth, we estimate this time $T_{\mathrm{severe}} = N\Delta t$ as the product of the number of events $N = T\omega$ over a fixed long-term observation period T and the time interval Δt spent above μ_2 after each exacerbation of given magnitude
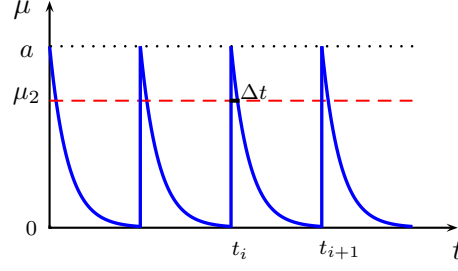
Figure S1. Schematic of the inflammatory status dynamics μ (solid) given by (S5) for large IR and $a > \mu_2$. Dashed red line indicates the "severe" inflammatory threshold μ_2; thick black solid denotes the time-interval Δt spent above the threshold.

$a > \mu_2$. The growth isoline of total ASM cell population $s(T) = \mathrm{const}$ (see Figs 4 and 6a) can thus be approximately characterised by $T_{\mathrm{severe}}/T \equiv \omega \, \Delta t = \mathrm{const}$. In particular, for a single exacerbation, from (S5) we have $\mu_2 \approx a \, \mathrm{e}^{-\mathrm{IR}\,\lambda_p\,\Delta t}$, and the time interval is $\Delta t \approx (\lambda_p \, \mathrm{IR})^{-1} \log \frac{a}{\mu_2}$, subject to the compatibility condition $(0 < \Delta t \ll \omega^{-1})$. The isoline of the ASM population growth for fast inflammation resolution is thus given by

$$\mathrm{IR} \approx A \left(\frac{\omega}{\lambda_p} \right) \log \left(\frac{a}{\mu_2} \right), \quad \mathrm{IR} \gg 1, \tag{S6}$$

where a/μ_2 and ω/λ_p are the relative magnitude and mean frequency of exacerbations respectively, and $A \equiv T/T_{\mathrm{severe}} \geq 1$ is a constant that defines the value of the fold-increase in ASM population size. The predicted growth isoline (S6) is plotted as the dashed white lines in Figure 4.